# Simulation of Steam Reforming Tube with Shaped Particles

A.P. Kagyrmanova*, N.V. Vernikovskaya, I.A. Zolotarsky, E.I. Smirnov, V.A. Kuzmin

Boreskov Institute of Catalysis SB RAS, Pr. Akad. Lavrentieva 5, 630090 Novosibirsk, Russia

## Abstract

Shaped catalysts are widely used in steam reforming. A comprehensive mathematical model able to predict and compare performance of different shaped catalysts is developed. The two-dimensional pseudo homogeneous model accounts for heat transfer between the tube wall and catalyst bed, conductivity and diffusivity in the radial direction in the packed bed and intraparticle diffusion. Gas volume changing caused by reaction stoichiometry results in a radial convective mass flux. A verification of the model and simulated performance of different shaped catalysts in steam reforming of natural gas are presented.

## Nomenclature

$C_i$, $C_i^{surface}$ – mole concentration and surface mole concentration component $i$, mole/m³

$C_{pi}$, $C_p$ – heat capacity component $i$ and total heat capacity, J/(mole·K)

$D_r$ – effective radial diffusivity of the bed, m²/s

$F$ – radiant surface area coefficient

$\Delta H_j$ – enthalpy change of reaction $j$, J/mole

$J_i$ – molar flux diffusivity of component $i$

$k_1$, $k_3$ – rate coefficients of reaction 1, 3, mole·atm$^{0.5}$/(m³·s)

$k_2$ – rate coefficient of reaction 2, mole/(m³·s)

$K_1$, $K_3$ – equilibrium constants for reactions 1, 3, atm²

$K_2$ – equilibrium constant of reaction 2

$K_i$ – adsorption constants of component $i$, atm$^{-1}$

$l$ – tube length coordinate, m

$P_i$, $P$ – partial pressure of component $i$ and pressure, atm

$R$ – gas constant, atm m³/(mole·K)

$r$ – tube radius coordinate, m

$T$, $T_w$ – temperature and wall tube temperature,

$\overline{u_l}$ – axial gas velocity under n.c., m/s

$\overline{u_r}$ – radial gas velocity under n.c., m/s

$y_i$ – mole fraction component $i$

$\gamma_{ij}$ – stochiometric coefficient component $i$ in reaction $j$

$\lambda_r$ – effective radial thermal conductivity of the bed , J/(m·s·K)

$\sigma$ – Stefan-Boltzmann coefficient, W/(m²·K⁴)

$\varepsilon$ – bed porosity

$\nu$ – gas viscosity, m²/s

$\omega_1$, $\omega_2$, $\omega_3$ – reaction rates of 1, 2, 3, mole/(m³·s)

$\varpi_j$ – apparent reaction rate, mole/(m³·s)

$\rho$ – pellet radius, m

$\rho_{gas}$ – gas density, kg/m³

$\rho_{ap}$ – apparent catalyst density, kg/m³

$\xi = 1.5$ – tortuosity

$Pe_h$ – Pecle number

$Pr$ – Prandtl number

$Sc$ – Shmidt number

*Subscripts*

*core* – bed core

*grain* – catalyst pellet

*gas* – gas phase

## Introduction

The catalytic steam reforming of natural gas is the main way to the production of ammonia, methanol and hydrogen for over 50 years. The steam reformer of a modern ammonia or methanol plant is a most expensive item of the plant and its improvement is very important to decrease final product costs.

The steam reforming reaction is strongly endothermic and typically it takes place in the tubes at temperatures 800-900°C and pressures ranging from 20 to 30 bars. Consequently, a furnace must be used to provide necessary reaction heat, whereas nickel based catalyst is loaded in furnace tubes made of very expensive nickel/chromium alloys. Thus, combination of catalytic reaction and heat transfer process determine the reformer efficiency and safety.

Last years application of shaped catalysts in steam reforming tubes became prevailing and a number of

*corresponding  authors. E-mail: aigana@catalysis.nsk.su

companies started marketing of catalyst with improved shape. Transition from regular catalysts to shaped ones allows to increase apparent catalyst activity; to enhance heat transfer; to reduce pressure drop along a tube. The best known catalysts for steam reforming are produced by Johnson Matthey Catalysts, UK (four – hole pellet, quadrolobe), Haldor Topsoe, Denmark (seven-hole pellet), Sud-Chemie, Germany (wheels), but the optimal catalyst shape for a given process is still debatable.

Many studies on a mathematical modeling of steam reformers [1-4] use models of various levels of complexity. Elnashaie S.S. *et al.* [3,4] carried out modeling of diffusion-reaction in porous catalyst, but for simulation of steam reformer tube they used one-dimensional model assuming that concentration and temperature gradients in the bed occur only in the axial direction. Grevskott S. *et al.* [2] carried out a simulation based on two-dimensional model of catalytic fixed-bed reactor coupled with the furnace chamber, but they did not account transport phenomena in porous catalyst. Most of these models are simplified, heat transfer parameters being not well defined, especially for shaped catalyst.

Recently developed theory for a prediction of radial heat transfer properties of beds packed by shaped particles [5,6] allows to estimate and to compare performance of such catalysts.

In present work original mathematical model of a single reformer tube based on two-dimensional model with additional space inside a catalyst particle is elaborated. The model accounts for the following heat and mass transfer phenomena: heat transfer between the tube wall and catalyst bed, conductivity and diffusivity in the radial direction in the packed bed and intraparticle diffusion. Among original features of the model there are: (i) a detailed accounting for a volume change caused by reaction stoichiometry resulted in a radial convective mass flux, (ii) Stephen-Maxwell equations for all components inside a catalyst particle instead of the convectional Fick's law for key components, (iii) additional mechanism of heat transfer by radiation, (iv) original model with a linear variation of radial thermal conductivity and diffusivity in the vicinity of the wall [5].

A verification of the suggested mathematical model is performed. Simulated performance of different shaped catalysts is presented and compared for parameters of a typical methanol plant steam reformer.

## Mathematical model

### Reaction Kinetics

The literature contains a large number of kinetic models for a steam reforming process [7-10]. Most of the reported kinetic rate equations are used at a narrow range of temperatures and pressures and do not account the rate of water-gas shift reaction. Xu and Froment [1] have developed more general and realistic rate equations for steams reforming that are used in this work. The intrinsic rate equations and constants were found by the authors [1] using integral flow reactor and commercial catalyst (Ni/MgAl$_2$O$_4$ spinel) with a fraction of 0.18-0.25 mm at temperatures 773-848 K and pressures ranging within 3-15 bar.

Rate expressions for a reaction network consisting of three representative reactions for steams reforming of natural gas were obtained:

$$CH_4 + H_2O = CO + 3H_2 \qquad (1)$$

$$CO + H_2O = H_2 + CO_2 \qquad (2)$$

$$CH_4 + 2H_2O = 4H_2 + CO_2 \qquad (3)$$
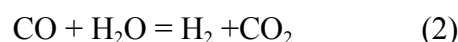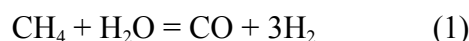
The corresponding rate expressions are:

$$\omega_1 = \left( \frac{k_1}{P_{H_2}^{2.5}} (P_{CH_4} P_{H_2O} - \frac{P_{H_2}^3 P_{CO}}{K_1}) / DEN^2 \right) \cdot \rho_{ap} \quad (4)$$

$$\omega_2 = \left( \frac{k_2}{P_{H_2}} (P_{CO} P_{H_2O} - \frac{P_H P_{CO_2}}{K_2}) / DEN^2 \right) \cdot \rho_{ap} \quad (5)$$

$$\omega_3 = \left( \frac{k_3}{P_{H_2}^{3.5}} (P_{CH_4} P_{H_2O}^2 - \frac{P_{H_2}^4 P_{CO_2}}{K_3}) / DEN^2 \right) \rho_{ap} \quad (6)$$

where

$$DEN = 1 + K_{CO}P_{CO} + K_{H_2}P_{H_2} +$$

$$+ K_{CH_4}P_{CH_4} + \frac{K_{H_2O}P_{H_2O}}{P_{H_2}} \qquad (7)$$

### Catalyst pellet model

A gas stream in steam reforming of methane consists of six components, reaction rates depending on concentrations of five components taking part in the reactions. The process in a catalyst pellet may be described by the following set of differential equations:

$$divJ_i = \sum_{j=1}^{3} \gamma_{ij}\omega_j \,, i = \overline{1,6} \qquad (8)$$

with boundary conditions:

$$\rho = 0: J_i = 0, \ i = \overline{1,6}$$

Due to considerable increase in a gas volume caused by reaction stoichiometry, the individual mass flux cannot be expressed using a simple Fick's law. Therefore, a general dusty gas model is used for deriving governing equation [11]:

$$-gradP_i = \frac{(RT)^2}{P} \sum_{\substack{k=1 \\ k \neq i}}^{N} \frac{C_k J_i - C_i J_k}{D_{ik}^*} + \frac{J_i RT}{D_i^{kn*}} \,,$$

$$i = \overline{1,6} \qquad (9)$$

where $D_{ik}^* = D_{ik}$ – effective binary diffusivity, $D_i^{kn*} = D_i^{kn}$ – effective Knudsen diffusivity, – permeability, $D_{ik}$ – binary diffusivity, $D_i^{kn}$ – Knudsen diffusivity.

After some transformations of equation (9), we obtain the expression for individual molar component flux:

$$J_i = -\cfrac{1}{\cfrac{RT}{P} \sum_{k=1}^{6} \cfrac{C_k}{D_{ik}^*} + \cfrac{1}{D_i^{kn*}}} gradC_i +$$

$$+ \cfrac{\cfrac{RT}{P} \sum_{k=1}^{6} \cfrac{J_k}{D_{ik}^*}}{\cfrac{RT}{P} \sum_{k=1}^{6} \cfrac{C_k}{D_{ik}^*} + \cfrac{1}{D_i^{kn*}}} C_i, \ i = \overline{1,5} \qquad (10)$$

where $D_{ri}^* = \cfrac{1}{\cfrac{RT}{P} \sum_{k=1}^{6} \cfrac{C_k}{D_{ik}^*} + \cfrac{1}{D_i^{kn*}}}$ is a diffusivity of a component $i$ through other components of the mixture, and $V_i^* = \cfrac{\cfrac{RT}{P} \sum_{k=1}^{6} \cfrac{J_k}{D_{ik}^*}}{\cfrac{RT}{P} \sum_{k=1}^{6} \cfrac{C_k}{D_{ik}^*} + \cfrac{1}{D_i^{kn*}}}$ is a hydrodynamic velocity of a component $i$.

The flux for the inert is equal to zero $J_{N_2} = 0$ as (i) nitrogen does not participate in reactions and its gradient is equal to zero, (ii) the fluxes for all components are symmetrical about the center of the pellet and are equal to zero in the center.

It is known [12] that effectiveness factor is almost coinciding for different shaped pellets (slab, infinite cylinder, spherical particles) if the ratio of volume to external surface area is equal. Due to this fact, the catalyst with slab geometry ($\rho_{grain} = V/S$) is used for a pellet modeling and a resulting mass balance of the $i$-th component can be presented by the following equation:

$$\frac{\partial}{\partial \rho}\left(D_{ri}^* \frac{\partial C_i}{\partial \rho}\right) - \frac{RT}{P}\frac{\partial}{\partial \rho}(V_i^* C_i) = \sum_{j=1}^{3} \gamma_{ij}\omega_j \,,$$

$$i = \overline{1,5} \qquad (11)$$

The concentration for the nitrogen we get from the mass balance:

$$C_{N_2} = C - \sum_{i=1}^{5} C_i \qquad (12)$$

where $C$ is a total molar concentration obtained from the equation $-\frac{\partial C}{\partial \rho} = \sum_{i=1}^{6} \frac{J_i}{D_i^{kn*}}$, which have been resulted from the expression (9) by its summation per $i = \overline{1,6}$.

Since in industrial steam reforming conditions the external mass transfer resistances are negligible the following boundary conditions can be used:

$$\rho = 0: \frac{\partial C_i}{\partial \rho} = 0, \ i = \overline{1,5}$$

$$\rho = \rho_{grain}: \ C_i = C_i^{surface}, \ i = \overline{1,6}$$

The apparent reaction rate is defined as:

$$\varpi_j = \frac{1}{\rho_{grain}} \int_0^{\rho_{grain}} \omega_j(\rho)d\rho \qquad (13)$$

*Mathematical model of a reformer tube*

The heat and mass balance equations in the reformer tube and corresponding boundary conditions are as follows:

$$\frac{P_0}{RT_0}\frac{\partial(\overline{u_l}y_i)}{\partial l} + \frac{1}{r}\frac{P_0}{RT_0}\frac{\partial}{\partial r}(r\overline{u_r}y_i) -$$

$$- \frac{1}{r}\frac{\partial}{\partial r}\left(r\frac{PD_r}{RT}\frac{\partial y_i}{\partial r}\right) = \sum_j (1-\varepsilon)\gamma_{ij}\varpi_j \,, i = \overline{1,5} \quad (14)$$

$$\frac{P_0}{RT_0}\overline{u_l}C_p\frac{\partial T}{\partial l} + \frac{P_0}{RT_0}\overline{u_r}C_p\frac{\partial T}{\partial r} - \frac{1}{r}\frac{\partial}{\partial r}\left(r\lambda_r\frac{\partial T}{\partial r}\right) -$$

$$- \sum_i C_{Pi}\left(\frac{\partial T}{\partial r}\right)\frac{P}{RT}D_r\frac{\partial y_i}{\partial r} = -(1-\varepsilon)\sum_j \Delta H_j\varpi_j \quad (15)$$

Equations for radial and axial components of the gas velocity originated from the reaction stoichiometry are defined as:

$$\frac{\partial \overline{u_l}}{\partial l} = \frac{2RT_0}{R^2_{tube}P_0} \int_0^{R_{tube}} \sum_i \sum_j r(1-\varepsilon)\gamma_{ij}\varpi_j dr \quad (16)$$

$$\overline{u_r} = -\frac{RT_0}{P_0 r} \int_r^{R_{tube}} (1-\varepsilon)r \sum_i \sum_j \gamma_{ij}\varpi_j dr +$$

$$+ \frac{1}{r}\frac{\partial \overline{u_l}}{\partial l}(\frac{R^2_{tube}}{2} - \frac{r^2}{2}) \qquad (17)$$

The boundary conditions:

$$0 \le r \le R_{tube} \quad l = 0: \overline{u_l}(0,r) = \overline{u_0};$$

$$T(0,r) = T_{in}; y_i(0,r) = y_{in} \; i = \overline{1,6}$$

$$0 \le l \le L \quad r = 0: \frac{\partial y_i(l,0)}{\partial r} = 0; \frac{\partial T(l,0)}{\partial r} = 0$$

$$r = R_{tube}: \frac{\partial y_i(l, R_{tube})}{\partial r} = 0 \; i = \overline{1,5};$$

$$\overline{u_r}(l, R_{tube}) = 0$$

$$\lambda_r \frac{\partial T}{\partial r} = \alpha(T_w - T) \qquad (18)$$

This model (eqs. (14-17)) accounts for a radial heat and mass transfer, including a convective component and diffusion heat transfer in heat balance equation caused by the different heat capacities of diffusing components.

In this work the model with a linear variation of radial thermal conductivity $\lambda_r$ in the vicinity of the wall for the description of heat transfer $\alpha_w$ is used [5,6]:

$$\alpha = \frac{\lambda_{r_{core}}}{\delta[\ln(\lambda_{r\,core} / \lambda_{r_{s}gas}) - 1]} \qquad (19)$$

The proposed model suggests that in the packed bed core the convective radial thermal conductivity $\lambda_r$ does not depend on radial position but further it linearly decreases in the layer of thickness $\delta$ from $\lambda_{r\,core}$ to the gas thermal conductivity $\lambda_{r\,gas}$ at the wall. The thickness of the characteristic wall-region layer is defined as:

$$\delta = d_{eqv} = \frac{4 \cdot \varepsilon_{bed}}{a_o \cdot (1 - \varepsilon_{bed})} \qquad (20)$$

where $\varepsilon_{bed}$ – bed porosity, $a_0$ – specific surface area of one grain without accounting channels.

Such model allows predicting realistic gas temperature near the wall and as a result correct prediction of the reaction rates for different shaped catalysts in the wide range of Reynolds numbers and tube/particle ratios.

*Radial heat- and mass transfer for shaped catalyst*

Effective radial thermal conductivity in the fixed bed $\lambda_r$ is composed of the conductivity without flow, convective and radiation parts of the thermal conductivity:

$$\lambda_r = \lambda_{r_0} + \lambda_{r\,conv} + \lambda_{r\,rad} \qquad (21)$$

At the industrial conditions of steam reforming the convective part of the thermal conductivity $\lambda_{r\,conv}$ is dominant. For general case it is proportional to the gas velocity $U_l$ and the length of fluid mixing $L$. The gas flow in the shaped packed bed runs both around particles and through its channels. Especially for this case we proposed the hydrodynamic model for description of convective radial thermal conductivity in packed bed for different shaped catalysts with arbitrary number and form of channels [6].

Using equations for the hydraulic resistance in the bed packed with solid particles and in the channels makes it possible to calculate the velocities of the flow around the particle $u_{out}$ and the channels $u_{hole}$ from the system of equations:

$$\begin{cases} u_l = u_{out} \cdot \varepsilon_{bed} + u_{hole} \cdot (\varepsilon_{hole} \cdot (1 - \varepsilon_{bed})) \cdot \langle \cos\alpha \rangle \\ g_1 \cdot u_{hole} + g_2 \cdot u_{hole}^2 = \frac{\Delta P}{\langle \cos\alpha \rangle \cdot L} = \\ = f_1 \cdot u_{out} + f_2 \cdot u_{out}^2 \end{cases} \quad (22)$$

here $\varepsilon_{hole}$ – the porosity of the single particle due to channels; $\Delta P$ – the pressure drop over the distance $\langle \cos\alpha \rangle \cdot L$; $\alpha$ – the angle between the axis of the tubular reactor and the axis of the particles; $f_1, f_2$ – Ergun's coefficients [13]:

$$f_1 = 150 \cdot \left(\frac{1 - \varepsilon_{bed}}{\varepsilon_{bed}}\right)^2 \cdot \frac{\nu}{\rho_{gas} \cdot d_p^2} \qquad (23)$$

$$f_2 = 1.75 \cdot \frac{1 - \varepsilon_{bed}}{\varepsilon_{bed}} \cdot \frac{\rho_{gas}}{d_p} \qquad (24)$$

The coefficients $g_1$, $g_2$ are used to calculate the pressure drop in the particle channel [14]:

$$g_1 = 16\pi \cdot \frac{\mu}{d_{gidr}^2} \times \begin{cases} 1 \\ 0.89 \end{cases} \qquad (25)$$

where 1 if channels cross-section have a circular form and 0.89 if channels cross-section – squre or sector.

$$g_2 = \frac{\pi}{4} \cdot \frac{\rho_{gas}}{L} \cdot \left[ 1.75 \cdot \left( 1 - \frac{\varepsilon_{hole}}{N_{hole}} \right) \right] \quad (26)$$

The hydraulic diameter of the channel is defined as:

$$d_{gidr} = \begin{cases} \text{side of square} & \text{if channels cross - section have a squre form} \\ \text{diameter of hole} & \text{if channels cross - section have a circular form} \\ \dfrac{D_{sect}}{1 + N_{hole}/\pi} & \text{if channels cross - section have a sector form} \end{cases} \quad (27)$$

Here $D_{sect}$ – diameter of the circle that is formed by all sectors joined side by side and $N_{hole}$ – the number of channels in one particle.

Effective radial thermal conductivity in the fixed bed core is defined as:

$$\lambda_{r\,core} = \lambda_{r\,bed} + \frac{\lambda_{r\,gas}}{k} \cdot [\varepsilon_{bed} \, \mathrm{Re}_{out} +$$

$$+ \varepsilon_{hole}(1 - \varepsilon_{bed}) \, \mathrm{Re}_{hole}] \cdot \mathrm{Pr} + \lambda_{r\,rad} \quad (28)$$

where $\lambda_{r\,bed}$ – effective thermal conductivity with a stagnant fluid, $k$ – empirically determined parameter depending on the ratio of particles diameters and the bed:

$$k = \frac{8}{1.78} \cdot \left[ 2 - \left( 1 - \frac{2}{D/d_p} \right)^2 \right] \quad (29)$$

here $d_p$ – diameter of equivalent volume sphere, $\nu$ – gas viscosity.

Reynolds numbers $\mathrm{Re}_{out}$ and $\mathrm{Re}_{hole}$ are expressed through real velocities:

$$\mathrm{Re}_{out} = \frac{d_p u_{out}}{\nu}; \ \mathrm{Re}_{hole} = \frac{d_{hole} u_{hole}}{\nu}$$

Radiation part of radial thermal conductivity in equation (28) is defined as:

$$\lambda_{r\,rad} = 2F\sigma T^3 d_{eqv} \quad (30)$$

Effective radial diffusivity in the bed is defined analogously to the above mentioned model for effective radial thermal conductivity:

$$D_{r\,core} = D_{r\,bed} + \frac{D_{r\,gas}}{k} \cdot [\varepsilon_{bed} \, \mathrm{Re}_{out} +$$

$$+ \varepsilon_{hole}(1 - \varepsilon_{bed}) \, \mathrm{Re}_{hole}] \cdot Sc \quad (31)$$

where $D_{r\,bed} = \dfrac{D_{r\,gas} \cdot \varepsilon}{\xi}$ – diffusivity in the bed with stagnant fluid, $D_{r\,gas}$ – same gas diffusivity as in the $Sc$ in eq. (31).

It should be noted that the convective part of diffusivity is considerably higher then $D_{r\,bed}$ and effective radial diffusivity does not practically depend on the individual properties of substances.

*Solution algorithm*

Instead of solving the system of partial differential equations (11) with boundary conditions the following dynamic equations were solved until achieving steady state:

$$\varepsilon_3 \frac{\partial C_i}{\partial t} = \frac{\partial}{\partial \rho} \left( D_{ri}^* \frac{\partial C_i}{\partial \rho} \right) -$$

$$- \frac{RT}{P} \frac{\partial}{\partial \rho} (V_i^* C_i) + \sum_{j=1}^{3} \gamma_{ij} \omega_j, \ i = \overline{1,5} \quad (32)$$

with initial conditions: $t = 0$: $C_i^o = C_i^o(r)$, $i = \overline{1,5}$

and boundary conditions: $\rho = 0$: $\dfrac{\partial C_i}{\partial \rho} = 0$, $i = \overline{1,5}$

$\rho = \rho_{grain}$: $C_i = C_i^{surface}$, $i = \overline{1,5}$.

The method of lines was used for numerical treatment of the system (32). Discrete approximation of differential operators on the spatial variable (pellet radius) and functions of reactions were based on the mass conserving integro-interpolation method [15]. The integral form of equations (32) was applied in every interval $[\rho_{l-1/2}, \rho_{l+1/2}]$. The function of reactions in every equation (for example, in $i$-th equation) of the system (32) was presented as a sum of two terms,

one of them is linear part with respect to $i$-th component and the other is the remaining one. This procedure allows transferring singled out linear part to the diagonal of the system, this fact increases monotony of the system and provides non-negativity of concentrations [16]. Thus, a large system of nonlinear ordinary differential equations results.

The system of nonlinear ordinary differential equations was solved iteratively. As initial guesses of concentrations inside the pellet surface concentrations were used. To find the vector of molar fluxes equations (8) with boundary conditions were solved as initial-value problem. Then coefficients $D_{ri}^*$, $V_i^*$ and nonlinear part of the function of reactions were found. Thus, a linear system of ordinary differential equations was obtained. This system was solved using a second-order Rozenbroke algorithm with automatic choice of the integration step [17]. The apparent reaction rates were determined by means of eq. (13).

For mathematical modeling of the processes occurring in the reformer tube we need to solve the system of nonlinear differential equations (14-17) with boundary conditions. The method of lines and integro-interpolation method were also used for numerical treatment of the system. As a result, we obtained a large system of nonlinear ordinary differential equations on length, and for solving this system we used iterations and a second-order Rozenbroke algorithm with automatic choice of the integration step.

## Simulation Results

Numerical calculations were carried out for the industrial conditions of a steam reforming process. Parameters of a typical methanol plant steam reformer were used in the modeling. Operating process conditions and catalyst characteristics are listed in the Table 1.

Parametric investigations on a single catalyst pellet are carried out using the dusty gas model (eqs. (11-13)) coupled with a model of the tube (eqs. (14-17)). This model allows one to obtain the concentration difference between the center and the surface of the catalyst particle at any position of the tube, as well as reaction rate from the catalyst surface as a function of the particle size, the component concentrations and temperatures on the outer particle surface and the effective diffusion coefficients.

The effectiveness factor $\eta$ was used as a measure for diffusion resistances and has been defined by apparent and intrinsic rates of methane consumption:

$$\eta = \frac{(\varpi_1 + \varpi_3)}{(\omega_1 + \omega_3)} \qquad (33)$$

where $\varpi_1, \varpi_3$ – apparent rates of reactions, $\omega_1$, $\omega_3$ – intrinsic rates of reactions at external surface conditions of the catalyst pellet.

**Table 1**
Operating conditions used in the modeling

| | |
|---|---|
| Inlet temperature | 520°C |
| Inlet pressure | 25 atm |
| Tube length | 12 m |
| Tube diameter | 0.102 m |
| Gas velocity | 9.9 m/s |
| Tube wall temperature | 880°C |
| Gas composition | |
| $CH_4$ | 24.4 vol.% |
| $H_2O$ | 73.0 |
| CO | 1.6 |
| $H_2$ | 1.3 |
| $CO_2$ | 0.01 |
| $N_2$ | 0.28 |
| Catalyst characteristics | |
| Density | 2030 kg/m³ |
| Permeability | 0.168 |

Figure 1 demonstrates dependence of size particle on the effectiveness factor at different operating process conditions on the outer catalyst surface, which correspond to different grain positions at the tube. Temperature growth causes increase in reaction rates of methane consumption $\omega_1$ and $\omega_3$ which proceeding promptly in the thin layer of catalyst surface while the component removal is limited by diffusion. Thus, the diffusion limitations in the small size particles (0.4 mm) and in the low temperature region (600 K) have been already observed; they are pronounced with increasing temperature and size particle, as shown in Fig. 1.

Figure 2 shows the methane concentration intraparticle profiles in the commercial catalyst with equivalent pellet radius of $\rho_{grain} = 1.99$ mm at four difference radius tube positions for the inlet tube distance
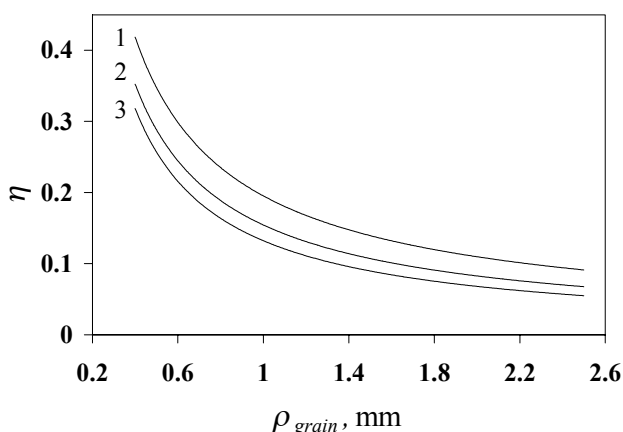
Process parameters: P = 25 atm; (1) T = 618°C: $y_{CH_4}$ = 0.171; $y_{H_2O}$ = 0.533; $y_{CO}$ = 0.009; $y_{H_2}$ = 0.2; $y_{CO_2}$ = 0.051; $y_{N_2}$ = 0.035; (2) T = 740°C: $y_{CH_4}$ = 0.099; $y_{H_2O}$ = 0.404; $y_{CO}$ = 0.043; $y_{H_2}$ = 0.358; $y_{CO_2}$ = 0.064; $y_{N_2}$ = 0.032; (3) T = 828°C: $y_{CH_4}$ = 0.047; $y_{H_2O}$ = 0.325; $y_{CO}$ = 0.084; $y_{H_2}$ = 0.456; $y_{CO_2}$ = 0.058; $y_{N_2}$ = 0.032.

Fig. 1. Effect of temperature and size pellet on the effectiveness factor.

$l$ = 1.56 m. The thickness of the catalyst layer taking part into reactions is only 0.65 mm and the gas composition at the center of the grain is close to equilibrium at corresponding temperature. The effectiveness factor for this catalyst pellets is approximately 0.07 for all positions along the tube radius.
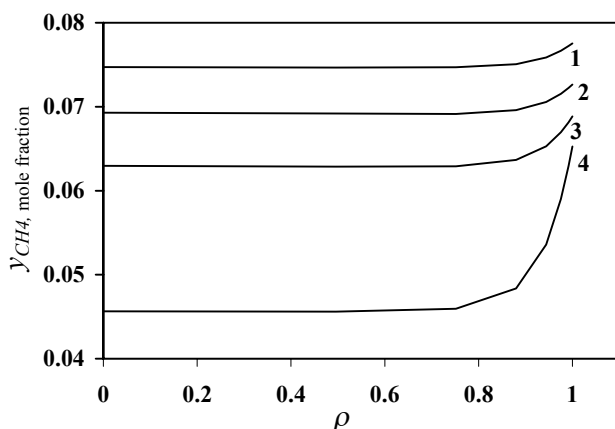


Process parameter: $\rho_{grain}$ = 1.99 mm; (1) tube centerline: T = 774°C: $y_{CH_4}$ = 0.077; $y_{H_2O}$ = 0.368; $y_{CO}$ = 0.059; $y_{H_2}$ = 0.401; $y_{CO_2}$ = 0.062; (2) T = 784°C: $y_{CH_4}$ = 0.072; $y_{H_2O}$ = 0.361; $y_{CO}$ = 0.062; $y_{H_2}$ = 0.410; $y_{CO_2}$ = 0.062; (3) T = 794°C: $y_{CH_4}$ = 0.069; $y_{H_2O}$ = 0.356; $y_{CO}$ = 0.066; $y_{H_2}$ = 0.417; $y_{CO_2}$ = 0.062; (4) tube wall: T = 824°C: $y_{CH_4}$ = 0.065; $y_{H_2O}$ = 0.351; $y_{CO}$ = 0.069; $y_{H_2}$ = 0.425; $y_{CO_2}$ = 0.061.

Fig. 2. Methane concentration profiles within the dimensionless catalyst pellet radius $\rho$ at the different radius tube positions for the inlet tube distance $l$ = 1.56 m.

Calculations showed that the term $(V_i^* C_i)$ in the mass balance equation (11) for catalyst pellet caused by hydrodynamic velocity of components as a result of reactions is insignificant and can be negligible for the real process operation conditions. The results assuming $(V_i^* C_i) = 0$ in equation (11) are almost identical to those calculated by the complete model.

Parameter $U_r$ in mass and heat balance in the tube model characterizes the fluctuating velocities in the radial tube direction caused by reaction stoichiometry. Figure 3 shows typical radial velocity profiles for different catalyst bed lengths. The values of radial velocities are negative due to the gas flow movement in the direction from the wall to the center of the tube. The maximum radial velocity values were 20-10 mm/s and were observed in the beginning of the catalyst bed where the reaction rates are sufficiently high. Further down the tube, radial velocity values are decreasing along the tube length and approaching to zero.
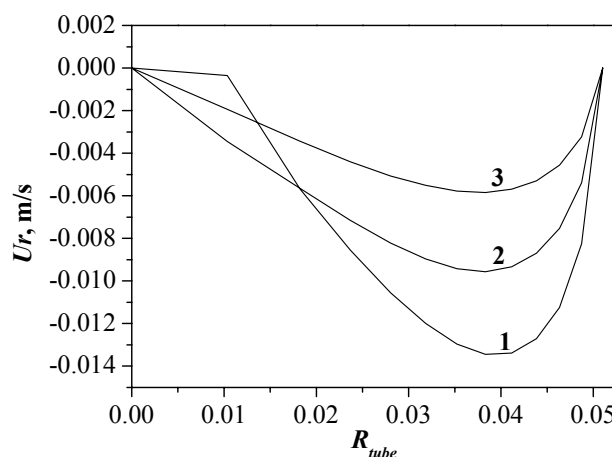


Fig. 3. Radial gas velocity profiles at the different length tube position: (1) $l$ = 0.6 m; (2) $l$ = 1.2 m; (3) $l$ = 1.8 m.

Essential contribution of terms responsible for radial convective transport of mass and heat transfer was determined. The term $\dfrac{1}{r}\dfrac{P_0}{RT_0}\dfrac{\partial}{\partial r}(r\overline{U_r}y_i)$ in mass balance equation (14) indicates the "convection of the radial flux". The term $\dfrac{P_0}{RT_0}\overline{U_r}Cp\dfrac{\partial T}{\partial r}$ in heat balance equation (15) is caused by the influence of the chemical reaction on the energy transport. To clarify the importance of each term, calculations were car-

ried out for the model equations (14) and (15) with artificially neglected $U_r$, *i.e.* $U_r = 0$ in (14) was set to zero and for the simplified model neglecting t influence of the radial convective heat and mass transport. Figure 4 shows that with such assumptions the predictions of the model neglecting convection of radial flux in mass balance equation (14) and the simplified model are closer and the maximum temperature difference is less than 1°C. At this time the results of calculations demonstrated that the difference between complete and simplified model is caused

by both terms. The term $\dfrac{1}{r}\dfrac{P_0}{RT_0}\dfrac{\partial}{\partial r}(r\overline{U_r}y_i)$ causes a

decrease in the effective radial heat transport, whe-

reas $\dfrac{P_0}{RT_0}\overline{U_r}Cp\dfrac{\partial T}{\partial r}$ increases the heat transport. The

largest effect is caused by the influence of the radial convective flux on the transport parameters, *i.e.* the

term $\dfrac{1}{r}\dfrac{P_0}{RT_0}\dfrac{\partial}{\partial r}(r\overline{U_r}y_i)$ in equation (14).

The radiation contribution $\lambda_{r\,rad}$ to the radial thermal conductivity $\lambda_{r\,core}$ in equation (28) is 4%.

The choice of catalyst pellet design for steam reforming is very important and has a significant effect on the reformer tube performance. Choosing the correct catalyst has a direct impact on apparent reaction rate, a heat transfer into the catalyst bed and a pressure drop along the tube.

The overall effect of catalyst pellet geometry on
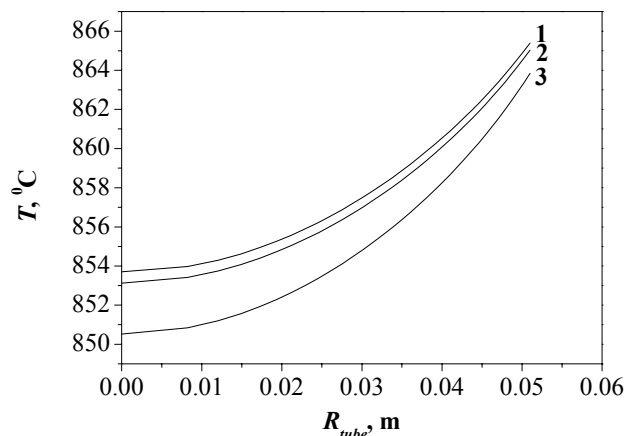


Fig. 4. Radial temperature tube profiles at the axial position $l = 2.4$ m and $\rho_{grain} = 1.99$ mm predicted by the (1) model without the radial convective term in mass balance, (2) simplified model and (3) complete model.

the performance of the reformer is shown in the simulation results presented in Table 2. Mathematical modeling of steam reformer tube packed by different shaped catalysts was carried out for parameters of a typical methanol plant reformer (Table 1). The trilobed catalyst for methane steam reforming was developed by Boreskov Institute of Catalysis [18]. Intrinsic activity of all catalysts was assumed to be the same. The characteristics of the catalyst presented in the Table 2 are relative to the trilobed catalyst. Degree of approaching equilibrium is a ratio of methane consumption at a fixed bed tube length ($l = 2.4$ m) to an equilibrium one at tube wall temperature ($y_{CH_4}/y^{eq}_{CH_4}$) and it can be used as a measure of methane conversion along the tube.

**Table 2**
Relative characteristics of shaped catalyst

| Catalyst type | Specific surface area | Degree of approaching equilibrium | Apparent heat transfer coefficient | Pressure drop |
|---|---|---|---|---|
| trilobed particle: outer diameter of each lobe: 9 mm, length: 20 mm, hole diameter: 4.5 mm | 1 | 1 | 1 | 1 |
| 4-hole cylinder: outer diameter: 14 mm, length: 19 mm, hole diameter: 3.6 mm | 1.14 | 1.06 | 0.84 | 0.90 |
| 7-hole cylinder: outer diameter: 20 mm, length: 13 mm, hole diameter: 4.3 mm | 1.10 | 1.24 | 0.65 | 0.69 |

Figure 5 shows the effectiveness factor along the tube calculated for different shaped catalysts. It was shown above that the nature of steam reforming catalyst is that activity is substantially a direct function of the geometric surface area. The trilobed catalyst has the lowest specific surface area in comparison

with the other catalysts, so it has the lowest effectiveness factor. Nevertheless the methane conversion along the tube for trilobed catalyst is the highest among the presented catalysts, which is explained by its improved heat transfer parameters due to its shape and can be verify by the radial temperature profiles for the considered catalysts presented in Fig. 6.
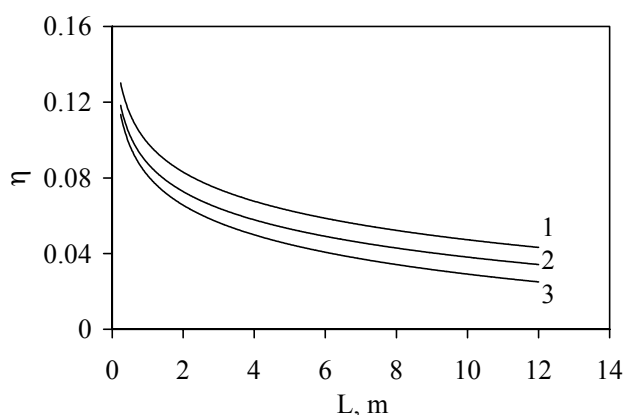


Fig. 5. Evolution of the effectiveness factor for different shaped catalysts: (1) 4-hole cylinder, (2) 7-hole cylinder and (3) trilobed particle.
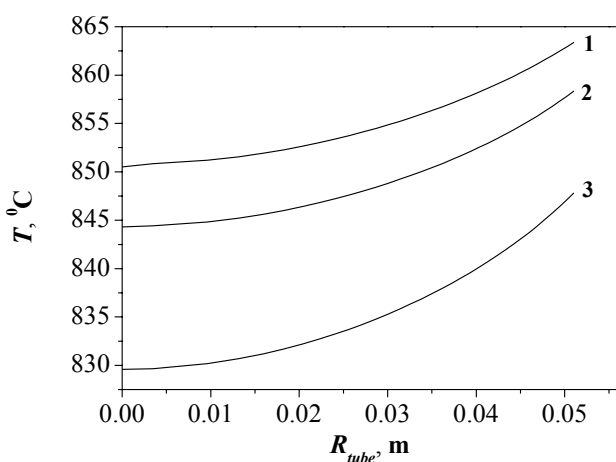


Fig. 6. Radial temperature profiles for different shaped catalysts at $l = 2.4$ m: (1) trilobed catalyst, (2) 4-hole cylinder and (3) 7-hole cylinder.

## Conclusions

The performance of a single tube packed by shaped particles of a commercial reactor for methane steam reforming was simulated numerically by means of the detailed two-dimensional pseudo-homogeneous model with additional space dimension inside a catalytic particle.

The process under industrial conditions is characterized by high diffusion limitations, that is, the reactions are completed in a thin shell near the catalyst pellet surface and temperature has a pronounced effect on the reactions. It was found that a hydrodynamic term in mass balance equation for a catalyst pellet is not significant in real process operation conditions. Essential contribution of terms responsible for radial convective transport of mass and heat was determined.

The original hydrodynamic approach to the description of heat and mass transfer parameters in packed bed of shaped particles with arbitrary number and form of channels was used to simulate and compare performance of steam reforming shaped catalysts for industrial conditions of a typical methanol plant reformer. The advantage of trilobed catalyst to diminish wall tube temperature was shown.

## Acknowledgements

## References

1. Xu, J., Froment, G.F., AIChE J. 35:88 (1989).
2. Grevskott, S., Rusten, T., Hillestad, M., Edwin, E. and Olsvik, O., Chem.Eng.Sci. 56:597 (2001).
3. Soliman, M.A., Elnashaie, S.S., Al-Ubaid, A. and Adris, A., Chem.Eng.Sci. 8:1801 (1988).
4. Abashar, M.E., Elnashaie, S.S., Math. Comput. Modelling, 7:85 (1993).
5. Smirnov, E.I., Muzykantov,A.V., Kuzmin, V.A., Kronberg, A.E., Zolotarskii, I.A., Chem. Eng.J., 11:243 (2003).
6. Smirnov, E.I., Muzykantov, A.V., Kuzmin V.A., Zolotarsky I.A., Koning, G.W., Kronberg, A.E., Chemistry for Sustainable Development, 11:293 (2003).
7. Hou, K., Hughes, R., Chem. Eng. J., 82:311 (2001).
8. Akers, W.W., Camp, D.P., AICh.J., 4:471 (1955).
9. Khomenko, A.A., Apel'baum, L.O., Shub, F.S., Kinetica i Kataliz (in Russian), 12:423 (1971).
10. Atroshchenko, V.I., Raman, Sh.K., Zvyagintsev, G.L. Him. Promyshlennost' (in Russian), 1:36 (1970).
11. Mason, E.A., Malinauskas, A., Gas Transport in Porous Media: The Dusty Gas Model, Elsevier, Amsterdam, 1983.

12. Rester, S., Jouven, J., Aris, A. Chem. Eng. Science, 24:1019 (1969).
13. Ergun, S. Chem. Eng. Prog.,48:89 (1952).
14. Vortuba, J., Mikus, O., Hlavacek, V., Skrivanek, J. Chem. Eng. Sci., 29:2128 (1974).
15. Samarskii, A.A., Mikhailov, A.P. Mathematical modeling Ideas. Methods. Examples, Moscow, 2001 (in Russian).
16. Rapatski, L.A., Yausheva, L.V, Preprint No1019, Novosibirsk, 1994 (in Russian).
17. Novikov, E.A. Numerical methods for solution of differential equations in chemical kinetics. In: Mathematical methods in chemical kinetics, Nauka, Novosibirsk, 1990 (in Russian).
18. Ivanova, A.S., Bobrova, I.I., Zolotarsky, I.A., Smirnov, E.I., Kuz'min, V.A., Noskov, A.S., Parmon,V.N. Russian patent application: from 26. 04.01 #2001111600.